Vision Research 51 (2011) 120–130

Contents lists available at ScienceDirect

Vision Research

journal homepage: www.elsevier.com/locate/visres

Spectral sensitivity of the photointrinsic iris in the red-eared slider turtle (*Trachemys scripta elegans*)

Grayson O. Sipe [a], James R. Dearworth Jr. [a,*], Brian P. Selvarajah [a], Justin F. Blaum [a], Tory E. Littlefield [a], Deborah A. Fink [a], Corinne N. Casey [a], David H. McDougal [b]

[a] Department of Biology and Neuroscience Program, Lafayette College, Easton, PA 18042, United States
[b] Laboratory of Autonomic Neurosciences, Pennington Biomedical Research Center, Louisiana State University System, Baton Rouge, LA 70808, United States

ARTICLE INFO

Article history:
Received 23 October 2009
Received in revised form 1 October 2010

Keywords:
Pupil
Photomechanical response (PMR)
Photopigment
Vitamin A_2
Cryptochrome

ABSTRACT

Our goal in this study was to examine the red-eared slider turtle for a photomechanical response (PMR) and define its spectral sensitivity. Pupils of enucleated eyes constricted to light by ~11%, which was one-third the response measured in alert behaving turtles at ~33%. Rates of constriction in enucleated eyes that were measured by time constants (1.44–3.70 min) were similar to those measured in turtles at 1.97 min. Dilation recovery rates during dark adaptation for enucleated eyes were predicted using line equations and computed times for reaching maximum sizes between 26 and 44 min. Times were comparable to the measures in turtles where maximum pupil size occurred within 40 min and possessed a time constant of 12.78 min. Hill equations were used to derive irradiance threshold values from enucleated hemisected eyes and then plot a spectral sensitivity curve. The analysis of the slopes and maximum responses revealed contribution from at least two different photopigments, one with a peak at 410 nm and another with a peak at 480 nm. Fits by template equations suggest that contractions are triggered by multiple photopigments in the iris including an opsin-based visual pigment and some other novel photopigment, or a cryptochrome with an absorbance spectrum significantly different from that used in our model. In addition to being regulated by retinal feedback via parasympathetic nervous pathways, the results support that the iris musculature is photointrinsically responsive. In the turtle, the control of its direct pupillary light response (dPLR) includes photoreceptive mechanisms occurring both in its iris and in its retina.

1. Introduction

1.1. Photointrinsic iris

Irises of several vertebrates can contract in response to light without feedback involving the retina (for review see Barr, 1989) and is defined as the photomechanical response (PMR). PMR in fish and amphibian has been studied since before the turn of the twentieth century (Armstrong & Bell, 1968; Barr & Alpern, 1963; Beer, 1894; Brown-Séquard, 1847; Glaus-Most, 1969; Guth, 1901; Kuchnow, 1971; Magnus, 1899; Seliger, 1962; Steinach, 1892; van Herk, 1928; von Campenhausen, 1963; Weal, 1956; Young, 1933; Morris, 1976; Nilsson, 1980; Rubin & Nolte, 1982; Barr, 1988; Douglas, Harper, & Case, 1998; Henning, Henning, & Himstedt, 1991), but much less has been reported for higher vertebrates such as mammal (Bito & Turansky, 1975; Lau, So, Campbell, & Lieberman, 1992; Zucker & Nolte, 1981) and bird (Pilar, Nunez, McLennan, & Meriney, 1987; Tu, Batten, Palczewski, & Van Gelder, 2004). Mechanisms underlying muscle contractions are thought to involve intracellular calcium and other secondary messengers amplified by G-protein cascades, which are triggered by photopigments, either by rhodopsin (Barr & Alpern, 1963; Barr, 1989; Barr & Gu, 1987; Bito & Turansky, 1975; Blaustein & Dewey, 1977; Kargacin & Detwiler, 1985; Lau et al., 1992; Rubin, Eller, & Nolte, 1986; Zucker & Nolte, 1978), melanopsin (Krivoshik & Barr, 2000; Kumbalasiri, Rollag, Isoldi, de Lauro Castrucci, & Provencio, 2007; Provencio, Jiang, De Grip, Hayes, & Rollag, 1998), or by the flavin-based cryptochrome (Tu et al., 2004).

1.2. Iris mechanism in reptiles

The iris mechanism in reptiles including alligator and turtle was described early as being similar to mammals using autonomic nervous control (Iske, 1929). Even so, pupil motility regulated by light intensity in the turtle was argued not to exist (Walls, 1942) and instead was thought to be governed solely by accommodation, which certainly plays a role (Henze, Schaeffel, Wagner, & Ott, 2004). In other reptiles such as snake constriction by the iris even has been

* Corresponding author. Fax: +1 610 330 5705.
E-mail address: dearworj@lafayette.edu (J.R. Dearworth).

0042-6989/$ - see front matter © 2010 Elsevier Ltd. All rights reserved.
doi:10.1016/j.visres.2010.10.012

suggested to compensate for the lack of a ciliary muscle by moving the lens forward during submersion in water (Fontenot, 2008). Experiments in turtle, however, clearly show a pupil controlled by parasympathetic innervations with slow light responsive dynamics (Dearworth et al., 2009; Granda, Dearworth, Kittila, & Boyd, 1995) and one that is weakly consensual (Dearworth et al., 2010). Instead of using a muscarinic cholinergic receptor site similar to mammal as was initially thought (Iske, 1929), turtle also uses the nicotinic subtype to contract the sphincter, a property more similar to bird (Dearworth, Cooper, & McGee, 2007). Sympathetic influence also affects pupil sizes in turtle suggesting presence of a dilator (Dearworth & Cooper, 2008), which was recently identified in sea turtle (Brudenall, Schwab, & Fritsches, 2008). Indeed, stimulation of the long ciliary nerve is able to generate observable pupil dilation (Dearworth et al., 2009). Irises in birds and reptiles including turtle were assumed to be only striated (Walls, 1942), but this too has come to be questioned since tissue in alligator (Reger, 1966) and other bird species (Nishida & Sears, 1970; Oliphant, Johnson, Murphy, & Howland, 1983) include smooth muscle.

1.3. Aim of study

An early study observed PMRs in reptilian vertebrates including turtle, but the iris movements were considered too slow and minimal to have any significant visual function (Barr, 1989; von Studnitz, 1933; Walls, 1942), and systematic analysis was never done. Our purpose in this study was to re-examine the iris in turtle for a photointrinisic response, compare it to the response measured in alert behaving animals, and then define its spectral sensitivity.

2. Methods

2.1. Animals

A total of ~135 turtles (*Trachemys scripta elegans*), ranging between 14.5 and 24.5 cm in carapace length and weighing between 0.40 and 2.14 kg, were purchased from Kons Scientific Co., Inc. (Germantown, WI). Maintenance of turtles and all procedures conformed to standards of the Institutional Animal Care and Use Committee (IACUC) at Lafayette College. Turtles were housed in a warm animal suite and placed in two 60 gallon tanks equipped with water filters. The capacity in each tank never exceeded 12 turtles. Sunning islands for animals were made of stacked bricks and were placed beneath 250 W heat lamps. Turtles were fed Rise floating fish diet (Pro-Pet, L.L.C., St. Marys, OH) daily, and the tanks cleaned once a week. Housing room was illuminated with time controlled lights that simulated natural day/night cycles at 14/10 h, light/dark, turning on at 6:00 AM and turning off at 8:00 PM. Using a radiometer (model DR-2000-LED, Gamma Scientific, San Diego, CA), radiant intensity from lights in the room was measured at 3.86×10^{-2} W cm^{-2} sr^{-1}. The temperature of the room was maintained at 22 °C.

2.2. Surgery

Turtles were first dark adapted for 30 min and then cryoanesthetized at 4 °C for 60 min (Fan, Scudder, & Ariel, 1997; Keifer & Houk, 1991; Maxwell, 1979). After this period, turtles were quickly decapitated and immediately pithed. Dissection was done quickly under a dim red light source, removing the eyelids and then the eyes from orbits. For initial experiments, the enucleated eyes were kept intact, and the light responses compared to alert behaving turtles. The majority of eyes used later in the experiment, however, were hemisected slightly posterior to the limbus to test for light responses occurring in the isolated iris, in the anterior part of the eye, and separated from the retina. Most of the experiments were completed within a few hours after dissection and during the day time of the housing room light cycle.

2.3. Apparatus

Both enucleated eyes, which were kept intact, and those which were hemisected were held within a small well and perfused with physiological turtle media (in mM: 96.5 NaCl, 2.6 KCl, 2.0 $MgCl_2$, 31.5 $NaHCO_3$, 20.0 D-glucose, and 4.0 $CaCl_2$). Media was adjusted to pH = 7.68, bubbled with 95/5% O_2/CO_2, and maintained at room temperature of 28 °C. Heat exchange from light sources to eyes was eliminated by shielding with fiber optic cables and infrared filters, and by continuous media perfusion, which was recycled to the eyes using a peristaltic pump (cf. Bito & Turansky, 1975).

2.4. Pupil measurements

Infrared sensitive cameras fitted with infrared light emitters were focused onto pupils to measure changes in the response to different light conditions. In experiments completed early in the study, images of the responses from enucleated eyes, which were kept intact, were captured from cameras and recorded onto video tape. To determine size, a ruler was placed in the same focal plane of the pupil. Horizontal pupil diameters were measured from still images, which were replayed onto a television monitor, using digital calipers with ±0.08 mm precision. Images from eyes of alert behaving turtles also were measured in this way.

For experiments done later with hemisected eyes, cameras were connected to a computer, utilizing the ViewPoint EyeTracker® software (Arrington Research, Inc., Scottsdale, AZ). Pupil measure was collected automatically with a precision of ±0.03 mm. The eye tracker detected the dark image of the pupil and used an ellipsoid algorithm to store the horizontal width (h) and vertical height (v). Data were imported from the file into Microsoft® Excel (Microsoft Corporation, Redmond, WA) to plot changes in horizontal pupil diameter or changes in pupil area. Pupil area was used to better measure range of movements for determining spectral sensitivity and was calculated using the formula for an ellipse, $\pi h \cdot v/4$ (cf. Granda et al., 1995).

2.5. Light stimulation

To compare responses of enucleated eyes to those measured from alert behaving turtles, experiments were done in a light integrating sphere of 40 cm (Dearworth & Cooper, 2008; Dearworth et al., 2007, 2009; Granda et al., 1995). Light source from a 150 W tungsten lamp was transmitted into the sphere by a fiber optic cable and mounted behind the line of sight of the turtles. Intensity was measured by radiometer and converted to the irradiance at the level of the iris, 1.38×10^{-3} J cm^{-2} s^{-1}, using the schematic of the eye for the red-eared slider turtle (Dvorak, Granda, & Maxwell, 1980; Northmore & Granda, 1991). Turtles were secured in a restraint that immobilized head movements, and then their heads were inserted into the sphere. When enucleated eyes were tested, they were positioned at the same location as where the head had been positioned. Infrared light emitting diodes, with emission peak of 915 nm, were mounted on each side for camera recordings.

Hemisected eyes were stimulated by diffuse light of broad-band spectra projected from a distance of 13 cm but without using a light integrating sphere. Light source was transmitted through a fiber optic cable. Irradiance of light was 5.70×10^{-4} J cm^{-2} s^{-1}. With a red long-pass filter having cut-on wavelength at 610 nm (filter No. 59512), irradiance was 3.58×10^{-4} J cm^{-2} s^{-1}. Using a blue

broad-band filter with peak transmission of 445 nm (Newport Stratford, Inc., filter No. 59830, Stratford, CT), irradiance was 1.79×10^{-5} J cm^{-2} s^{-1}. The light protocol for measures in alert behaving turtles, enucleated eyes, and hemisected eyes, which were stimulated with broad-band filters, began with 10 min of light adaptation, then either 40 or 50 min of dark adaptation, and a return to 10 min of light adaptation to test for tissue viability.

For a second set of experiments, narrow-band filters with full width at half maximum (FWHM) of 10 nm (Edmund Industrial Optic, Barrington, NJ) were used to determine spectral sensitivity. Filters having the following nominal wavelengths were tested: 410, 430, 480, 520, 580, and 640 nm. At each wavelength, neutral density filters (Newport Stratford Inc., Stratford, CT) were used to attenuate intensities. Irradiance was converted to log quanta using nominal wavelength of each filter. To test higher intensities of light, a 300 W quartz halogen lamp also was used and filtered for infrared emissions. A fan was used to blow heat away from the preparation to maintain the temperature at 28 °C.

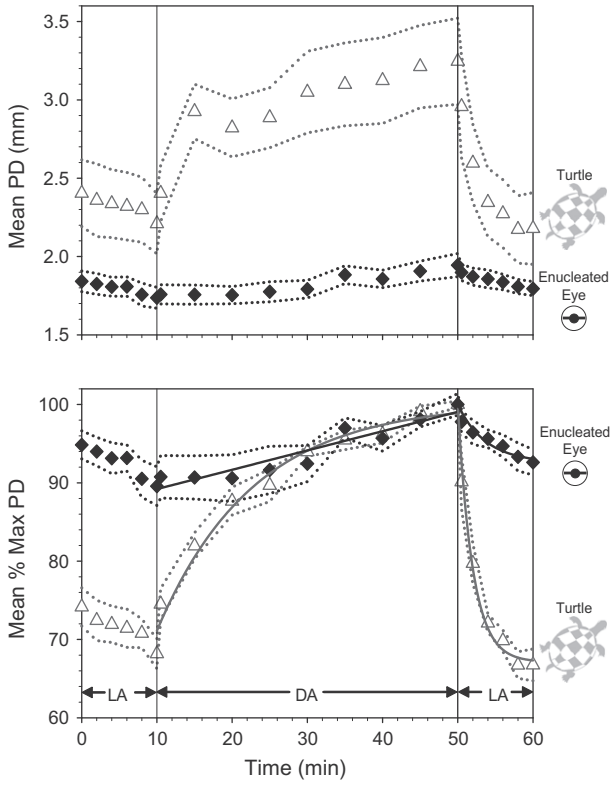

Fig. 1. Mean pupillary light responses for alert behaving turtles ($N = 6$, white triangles) compared to responses from enucleated eyes ($N = 6$, black diamonds). Ten minute of light adaptation (LA) at irradiance 1.38×10^{-3} J cm^{-2} s^{-1} preceded and followed 40 min of dark adaptation (DA). In top graph, mean pupil diameters (PD) ± standard errors (dotted lines) are plotted. In bottom plot, responses are normalized to maximum pupil diameters. Time constant equations were fit to data from turtles (gray curves) during both DA and second LA. A time constant equation also was fitted to data during LA for enucleated eyes (black curve); however, a linear equation (black line) better fit dilation during DA.

2.6. Data analysis

Means with standard errors (SE) were normalized to maximum pupil sizes and plotted as a function of time. Analysis of variance (ANOVA) and *t*-tests were used to test the statistical significance of changes, which were established at levels of $P < 0.05$. For each trial, pupilloconstrictions to narrow-band filters were determined by subtracting the percent maxima measured during the last 5 min of light adaptation from those measured during the last 5 min of dark adaptation. Means for each wavelength were plotted as a function of irradiance and analyzed using SigmaPlot (SPSS Inc., Chicago, IL). Hill equation, pupilloconstriction = $a\,[I^b/(I^b + c^b)]$, was used to determine relative sensitivity, where I is irradiance, a is maximal pupilloconstriction, b is a constant, and c is the irradiance at which half-maximal pupilloconstriction is produced (Gamlin et al., 2007; Peirson, Thompson, Hankins, & Foster, 2005). Sensitivity curves were generated by plotting log reciprocal of c versus nominal wavelengths for each filter. Values were normalized to maximum response and compared to nomograms of photopigments. Data were also best fit by least sum square method to vitamin A_1 and A_2 templates using polynomial equations, which approximate cone photopigment spectral sensitivity fundamentals (Baylor, Nunn, & Schnapf, 1987; DeMarco, Pokorny, & Smith, 1992; Govardovskii, Fyhrquist, Reuter, Kuzmin, & Donner, 2000). Goodness-of-fits were compared by the profile-fitting error (PFE), equal to ratio between sum of squared residuals and sum of squared observed responses (Dearworth & Granda, 2002; Sun & Bonds, 1994).

The rates for pupilloconstriction in response to light stimulations and the dilations for intact turtles were determined by a rise to maximum time constant equation, $y = y_0 + a(1 - e^{-t/\tau})$, where y is pupil size, y_0 is offset pupil size, a is maximum pupillary change, t is time, and τ is time constant (Clarke, 2007; Dearworth & Cooper, 2008; Dearworth et al., 2007, 2009, 2010; Granda et al., 1995). Pupillary dilations in enucleated and hemisected eyes were fit with a line equation, $y = mt + b$, where m is slope and b is the y-intercept.

3. Results

3.1. Responses in enucleated eye versus intact turtle

Pupil changes were greater in eyes of alert behaving turtles (Fig. 1, white triangles) than compared to enucleated eyes (Fig. 1, black diamonds); baseline in turtles was also larger than in enucleated eyes (Fig. 1, top plot). Turtles had pupils which dilated from 2.21 ± 0.19 (SE) mm at 10 min in light to 3.25 ± 0.27 mm at 50 min in dark (paired *t*-test, $P < 0.0003$). Pupils of enucleated eyes

Table 1
Summary statistics for responses to broad-band filters.

Preparation	Broad-band filter	Irradiance (J cm^{-2} s^{-1})	% Max PD versus time	DA_{Max} (100%)	1st LA_{Min}	2nd LA_{Min}	DA_{Max} versus 1st LA_{Min}	DA_{Max} versus 2nd LA_{Min}	1st LA_{Min} versus 2nd LA_{Min}
			ANOVA *P* values	±SE	% ± SE	% ± SE	*t*-test *P* values	*t*-test *P* values	*t*-test *P* values
Intact turtle	White	1.38×10^{-3}	<0.01	±0.44	68.18 ± 1.89	66.73 ± 1.70	<0.0001	<0.0001	0.42
Enucleated eye	White	1.38×10^{-3}	<0.01	±1.38	89.57 ± 2.47	92.61 ± 1.63	<0.005	<0.005	0.09
Hemisected eye	White	5.70×10^{-4}	<0.0001	±0.28	92.56 ± 0.83	93.04 ± 1.07	<0.0001	<0.0001	0.59
Hemisected eye	Red	3.58×10^{-4}	<0.003	±0.57	90.31 ± 2.78	94.22 ± 1.65	<0.05	0.06	0.22
Hemisected eye	Blue	1.79×10^{-5}	<0.0001	±0.82	91.59 ± 1.72	92.19 ± 0.31	<0.03	<0.03	0.79

DA_{Max} (100%) = mean maximum pupil diameter during dark adaptation.
LA_{Min} = mean minimum pupil diameter during light adaptation.

Table 2
Fitted values of line and time constant equations for responses to broad-band filters.

Preparation	Broad-band filter	Dilation					Constriction		
		Y-intercept $b \pm$ SE (%)	Slope $m \pm$ SE (%/min)	Amplitude $a \pm$ SE (%)	Time constant $\tau \pm$ SE (min)	r^2	Amplitude $a \pm$ SE (%)	Time constant $\tau \pm$ SE (min)	r^2
Intact turtle	White	–	–	29.07 ± 1.92	12.78 ± 2.41	0.98	−32.89 ± 1.59	1.97 ± 0.29	0.99
Enucleated eye	White	89.20 ± 0.65	0.25 ± 0.03	–	–	0.90	−7.44 ± 1.18	3.70 ± 1.68	0.93
Hemisected eye	White	93.19 ± 0.24	0.11 ± 0.01	–	–	0.78	−8.05 ± 0.33	2.84 ± 0.32	0.99
Hemisected eye	Red	91.27 ± 0.28	0.20 ± 0.01	–	–	0.87	−5.48 ± 0.35	1.44 ± 0.21	0.97
Hemisected eye	Blue	89.78 ± 0.31	0.24 ± 0.01	–	–	0.89	−6.68 ± 0.70	1.47 ± 0.35	0.92

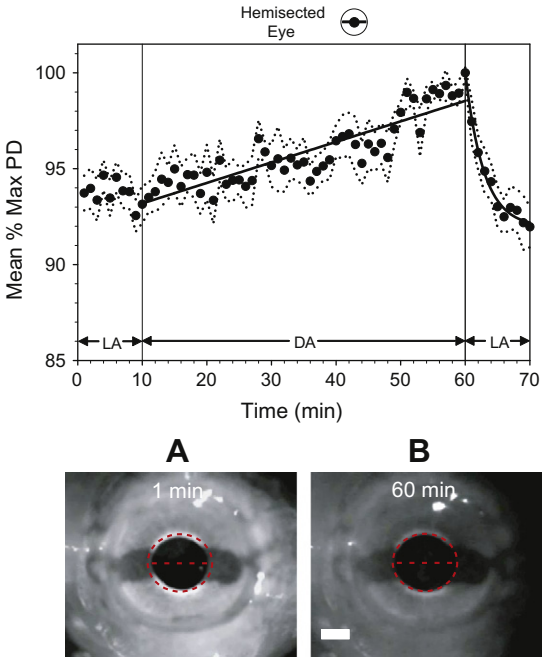

Fig. 2. Mean responses from hemisected eyes ($N = 10$). A linear equation (black line) fit the rate of dilation during DA. A time constant equation was used to fit constriction (black curve) during LA. Images of eyes at bottom are frame stills captured during LA at 1 min (A) and during DA at 60 min (B). Dashed red line with circle is fitted to pupil in (B) and superimposed on (A) for direct comparison. White scale bar = 1 mm. Pupil diameter in (A) is 1.88 mm and in (B) is 2.12 mm.

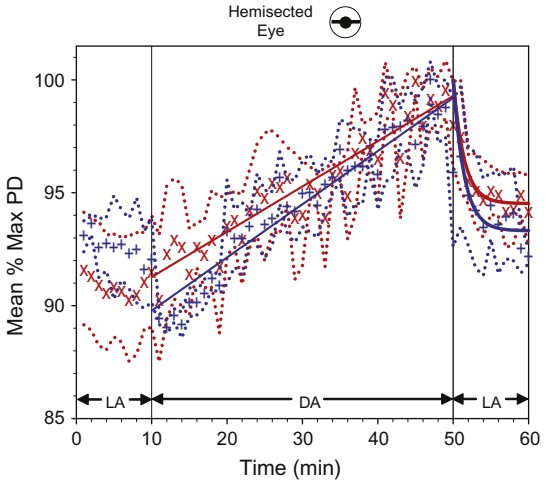

Fig. 3. Mean responses ($N = 3$) of hemisected eyes to red (×) and blue (+) broad-band filtered lights. Linear equations were fit to dilations during DA (red and blue lines), and time constant equations were fit to constrictions during second LA (red and blue curves).

also dilated but the change was less going from 1.74 ± 0.07 to 1.95 ± 0.07 mm ($P < 0.005$).

Fig. 1 (bottom) shows normalized responses. Pupils for both turtles and enucleated eyes dilated during dark adaptation and constricted during return to light adaptation (ANOVA, $P < 0.01$). For turtles, the maximum value during dark adaptation was significantly different than the minimum values during both the first and second light adaptation (paired *t*-tests, $P < 0.0001$) and showed that pupils changed by as much as 33.28%. When minimum values from first and second light adaptations were compared, they were not significantly different ($P = 0.42$). For enucleated eyes, change was less at 10.43%. The maximum value during dark adaptation also was significantly different than minimum values during first and second light adaptations ($P < 0.005$), but again minimum values from first and second light adaptations were not ($P = 0.09$). Table 1 summarizes the results of ANOVAs and *t*-tests.

For turtles, time constant equations (Fig. 1, bottom, gray curves) were fit to both dilation during dark adaptation ($a = 29.07 \pm 1.92\%$, $\tau = 12.78 \pm 2.41$ min, $r^2 = 0.98$) and to constriction during second light adaptation ($a = -32.89 \pm 1.59\%$, $\tau = 1.97 \pm 0.29$ min, $r^2 = 0.99$).

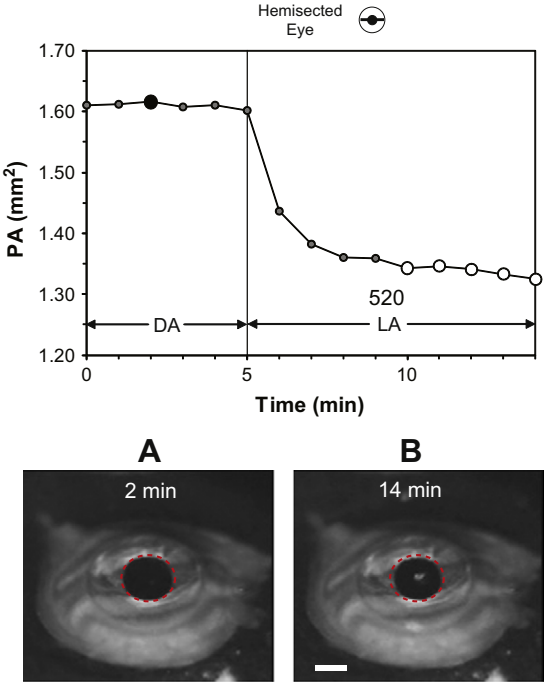

Fig. 4. Representative changes by pupil area (PA) from a hemisected eye stimulated with narrow-band filtered light at 520 nm. Pupil sizes during the last 5 min of LA (white round symbols) were used to determine mean pupilloconstrictions (cf. Fig. 7). Pupil sizes at 10, 11, 12, 13, and 14 min were subtracted from the maximum size (black round data symbol) occurring in the last 5 min of a 40 min period of DA. Images of eyes at bottom are frame stills captured during DA at 2 min (A) and during LA at 14 min (B). Dashed red ellipse is fitted to pupil in (A) and superimposed on (B) for direct comparison. White scale bar = 1 mm.

For enucleated eyes, a time constant equation (Fig. 1, black curve) also was fit to constriction during the second light adaptation ($a = -7.44 \pm 1.18\%$, $\tau = 3.70 \pm 1.68$ min, $r^2 = 0.93$), but a linear equation (Fig. 1, black line) fit dilation during dark adaptation better and was used instead ($b = 89.20 \pm 0.65\%$, $m = 0.25 \pm 0.03\%$/min, $r^2 = 0.90$). Table 2 summarizes the parameters used for the fits.

3.2. Responses of hemisected eyes to broad-band spectral lights

Pupils of hemisected eyes responded similarly to the enucleated eyes, which were kept intact (Fig. 2). White light at 5.70×10^{-4} J cm^{-2} s^{-1} constricted pupils during the first and second light adaptations, and dilation occurred during dark adaptation (Table 1, ANOVA, $P < 0.0001$). Change in pupil diameter was 7.44%. Linear equation was fit to dilation ($b = 93.19 \pm 0.24\%$, $m = 0.11 \pm 0.01\%$/min, $r^2 = 0.78$), and time constant equation was fit to constriction ($a = -8.05 \pm 0.33\%$, $\tau = 2.84 \pm 0.32$ min, $r^2 = 0.99$). Red and blue broad-spectral lights (Fig. 3) also constricted pupils during light adaptations with dilations occurring during dark adaptation (Table 1, ANOVA, $P < 0.003$). For responses to red light (Fig. 3, red ×) change in pupil diameter was 9.96%; for responses to blue light, change was 8.41% (Fig. 3, blue +). Overlap of SEs (Fig. 3, red and blue dotted lines) indicated that the responses were not statistically different and was further supported by results from ANOVA comparing the responses to each other ($P = 0.28$). Statistics were consistent with those obtained using white light except for one t-test, which was computed for red light, comparing maximum value during dark adaptation to minimum value for second light adaptation (cf. Table 1, $P = 0.06$). As before, linear and time constant equations (cf. Table 2) closely matched data.

3.3. Responses of hemisected eye to narrow-band filtered lights

Fig. 4 shows a representative response from a hemisected eye to 520 nm light at 13.85 log quanta cm^{-2} s^{-1}, 0 OD. Pupil area decreased from its maximum in the dark at 1.62–1.23 mm^2 in the light. The mean normalized responses to 520 nm and other wavelengths (410, 430, 480, 580, and 640 nm) are shown in Fig. 5. As light intensity was attenuated, pupil movements decreased.

The lowest light intensity producing a significant pupil change was 410 nm at 12.43 log quanta cm^{-2} s^{-1} (Table 3, 2.3 OD, ANOVA, $P < 0.003$). Reduction of pupil size increased with intensity and was greatest at 91.78% occurring at 13 min in response to 13.2 log quanta cm^{-2} s^{-1} (Fig. 5, trace for 1.3 OD). The change was nearly the same at 1.0 and 0.0 OD. Significant changes in pupil size also occurred for the other wavelengths but at intensities of about one log unit or higher, the lowest intensity at 13.31 log quanta cm^{-2} s^{-1} for 480 nm (Fig. 5, trace for 2.3 OD).

Time constant equations were fit to changes by pupil occurring during light adaptation (Fig. 6). The amplitudes (a) ranged from

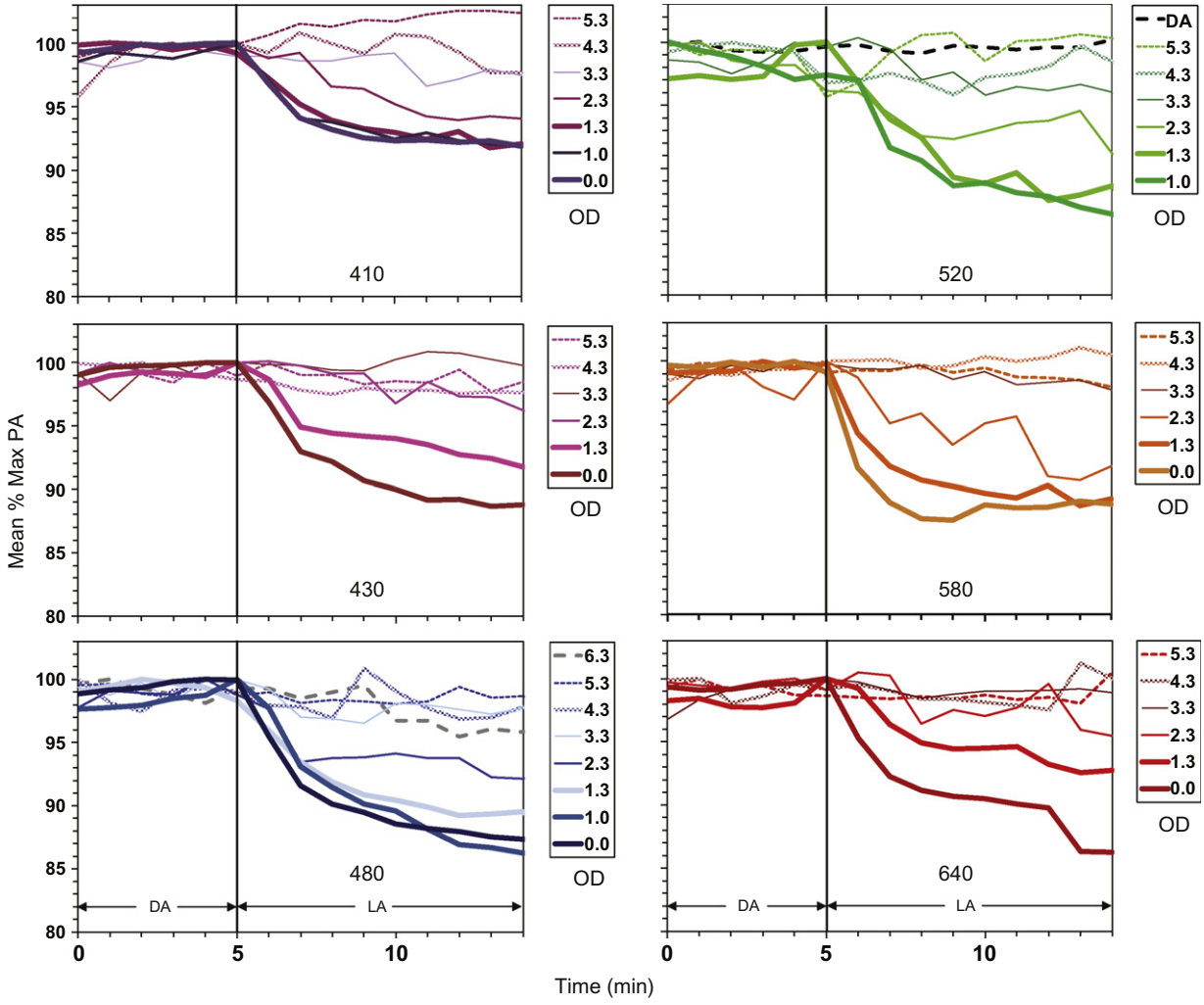

Fig. 5. Changes by normalized pupil area (PA) for hemisected eyes to six wavelengths (410, 430, 480, 520, 580, and 640 nm). Between 3 and 13 trials were tested at each of the different optical densities (OD) that are coded in legends to the right of the plots.

Table 3
Summary statistics for responses to narrow-band filters.

Narrow-band filters λ_n with 10 nm FWHM	Attenuated intensity	Irradiance	N	% Max PD versus time
	OD	Log quanta (cm^{-2} s^{-1})		ANOVA *P* values
410	0.0	14.69	5	<0.0003
	1.0	13.62	3	<0.01
	1.3	13.32	9	<0.0001
	2.3	12.43	6	<0.003
	3.3	11.44	6	0.68
	4.3	10.48	4	0.75
	5.3	9.30	4	0.10
430	0.0	14.97	4	<0.0001
	1.3	13.72	8	<0.05
	2.3	12.84	8	0.60
	3.3	11.85	4	0.99
	4.3	10.69	3	0.94
	5.3	9.40	10	0.75
480	0.0	15.47	5	<0.0001
	1.0	14.46	5	<0.0001
	1.3	14.18	7	<0.0001
	2.3	13.31	7	<0.0001
	3.3	12.38	5	0.69
	4.3	11.27	13	0.86
	5.3	10.14	11	1.00
	6.3	9.53	4	0.25
520	1.0	14.53	3	<0.0001
	1.3	14.32	6	<0.0001
	2.3	13.46	4	<0.03
	3.3	12.56	6	0.70
	4.3	11.47	8	1.00
	5.3	10.27	6	0.56
	DA	[a]6.93	6	0.97
580	0.0	15.77	5	<0.0001
	1.3	14.84	9	<0.03
	2.3	14.00	6	<0.05
	3.3	13.16	4	0.08
	4.3	12.16	4	0.99
	5.3	11.06	4	0.99
640	0.0	15.98	5	<0.03
	1.3	14.93	9	<0.003
	2.3	14.06	5	0.36
	3.3	13.28	5	0.49
	4.3	12.29	3	0.42
	5.3	11.35	10	0.99

λ_n = Nomimal wavelength.
FWHM = full width at half maximum.
DA = dark adaptation.
[a] Radiometer measure in total darkness.

−6.98% to −15.34%, and time constants (τ) ranged from 1.00 to 7.66 min. Table 4 summarizes parameters.

3.4. Irradiance thresholds

Hill equations were fit to pupilloconstrictions as a function of intensity at each wavelength to identify threshold irradiance values (Fig. 7). The threshold irradiance (c) was lowest for 410 nm at 12.29 log quanta cm^{-2} s^{-1} and highest for 640 nm at 14.88 log quanta cm^{-2} s^{-1}. Fits were done initially with the maximum pupilloconstriction (a = 12.48%) found at 480 nm. Slopes (b) for fits to 430 through 640 nm ranged from a low of 1.21 for 480 nm to high of 1.71 for 430 nm, matching the data well ($r^2 \geqslant 0.97$). When refitted using the average from their slopes, b = 1.52, the threshold values and r^2 did not significantly change. The slope for 410 nm, however, was considerably lower (b = 0.37), and the fit much poorer (r^2 = 0.58). The data for 410 nm was best fit instead using its own maximum pupilloconstriction (a = 7.81%). Table 5 summarizes the parameters.

4. Discussion

4.1. Range of response

Pupil of turtle remains partially responsive to light after denervation of the eye (Fig. 1) and confirms that the PMR, although slow, (von Studnitz, 1933) is present in the turtle. Compared to the direct pupillary light response (dPLR) in alert behaving turtles, which respond over ~33% range (Dearworth et al., 2009, 2010), the PMR in enucleated eyes responds one-third as much at ~11% (Fig. 1, bottom plot). Also of note is that the baseline size for enucleated eye is less compared to *in vivo* (Fig. 1, top plot), as is similarly observed for other *in vitro* preparations including cat (Distler & Hoffmann, 1986) and urodeles (Henning & Himstedt, 1994). The reason for difference is not clear but could be attributed to the lack of both sympathetic and parasympathetic drives going to the iris, leaving single control of iris movements to the PMR.

The amplitude of the PMR in turtle is similar to hooded rat, which is between 10% and 20% (Bito & Turansky, 1975), but less compared to most other non-mammals (Pilar et al., 1987; Seliger, 1962; Tu et al., 2004). In most mammals including human, the PMR have been assumed to be non-existent (Loewenfeld, 1993) with notable exception of hamster, which has amplitude that is nearly 70% (Bito & Turansky, 1975; Lau et al., 1992). The amplitude for the PMR is similar to the consensual pupillary light response (cPLR), also ~11% (Dearworth et al., 2010), but because of lack of trans-illumination, the cPLR must be a separate light response generated by neural innervations.

Fig. 8 shows a test to see if a simple mathematical operation, the adding of the PMR to the centrally neural mediated cPLR, could predict the dPLR (cf. Fig. 1). Although the 95% confidence limits do slightly overlap, the linear summing of the PMR to the cPLR (a = −19.67%) falls short of being able to account for all of the dPLR (a = −32.89%) and suggests that the photoreceptive mechanisms involved may augment each other in some non-linear fashion. Future experiments that define action spectra for both the dPLR and the cPLR and then compare them to action spectrum of the PMR could help identify interactions involved in this. Better understanding in turtle of the mechanisms coupling the light triggered photopigments to the muscle contraction involving calcium and how they interact with the traditional neural signals activating muscle contraction could also provide some insight.

4.2. Timing of response

Timing of the constriction by PMR in turtle is about two times slower (Tables 2 and 4) compared to other vertebrates in which constriction takes nearly 0.50 min to complete (Barr, 1989; Bito & Turansky, 1975; Douglas et al., 1998; Seliger, 1962; Tu et al., 2004). Timing of the dilation associated with the PMR is even slower. Given slopes ranging from 0.11% to 0.25%/min (Table 2), the time for a 11% change to occur requires between 26 and 44 min, almost one log unit slower than the timing in other animals (e.g., Bito & Turansky, 1975). In fact, timing is most similar to that observed for the PLR of turtle for which dilation, recovering from ~33% constriction, occurs with a time constant of 12.78 min and reaches maximum size within 40 min. The rate of dilation for enucleated eyes, however, clearly is different and better described using a linear function whereas for *in vivo* the change is exponential. The reason for difference again could be from the lack of parasympathetic and sympathetic opponent processes driving the pupil size (e.g., Lowenstein & Loewenfeld, 1950). Constriction by enucleated eyes, however, is still exponential due to contractions, which are amplified by light triggered intracellular cascades (e.g., Barr, 1989).

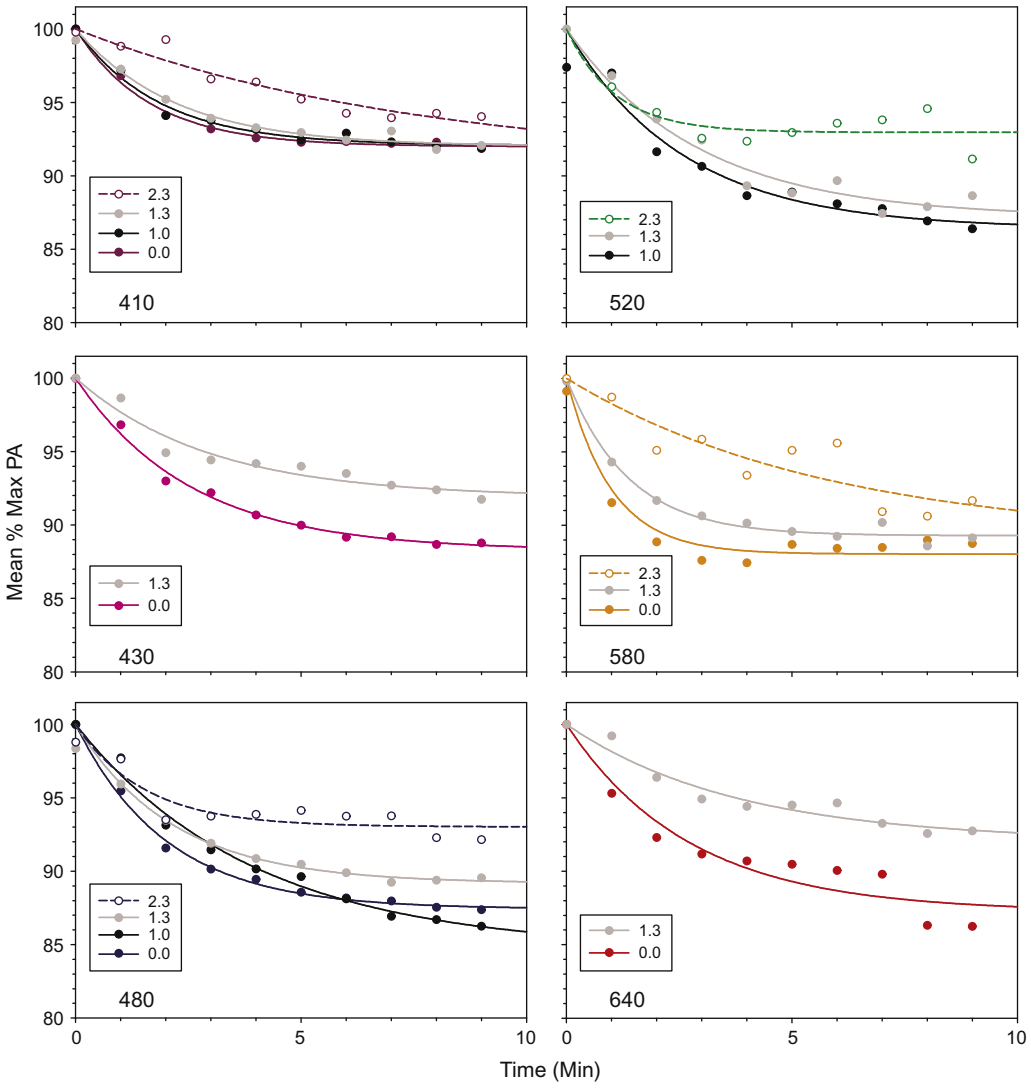

Fig. 6. Time constant equations fitted to changes by pupil area, which were statistically significant. Optical densities for those selected are coded in the legends.

Table 4
Fitted values for time constant equations for responses to narrow-band filters.

Narrow-band filters λ_n with 10 nm FWHM	Attenuated intensity (OD)	Constriction		
		Amplitude a ± SE (%)	Time constant τ ± SE (min)	r^2
410	0.0	−8.01 ± 0.25	1.65 ± 0.13	0.99
	1.0	−7.93 ± 0.41	1.86 ± 0.23	0.98
	1.3	−7.99 ± 0.46	2.22 ± 0.33	0.97
	2.3	−9.33 ± 3.44	7.66 ± 5.12	0.93
430	0.0	−11.72 ± 0.40	2.56 ± 0.24	0.99
	1.3	−8.11 ± 0.78	2.98 ± 0.80	0.95
480	0.0	−12.57 ± 0.31	2.01 ± 0.12	1.00
	1.0	−15.34 ± 0.91	3.94 ± 0.63	0.99
	1.3	−10.82 ± 0.67	2.16 ± 0.34	0.97
	2.3	−6.98 ± 1.07	1.51 ± 0.55	0.82
520	1.0	−13.59 ± 1.34	2.59 ± 0.69	0.92
	1.3	−12.83 ± 0.93	2.92 ± 0.59	0.97
	2.3	−7.04 ± 8.17	1.07 ± 1.19	0.49
580	0.0	−11.97 ± 0.98	1.00 ± 0.20	0.94
	1.3	−10.71 ± 0.47	1.37 ± 0.14	0.99
	2.3	−10.99 ± 4.45	5.84 ± 5.15	0.81
640	0.0	−12.74 ± 1.46	2.73 ± 0.86	0.91
	1.3	−7.94 ± 0.95	3.78 ± 1.24	0.95

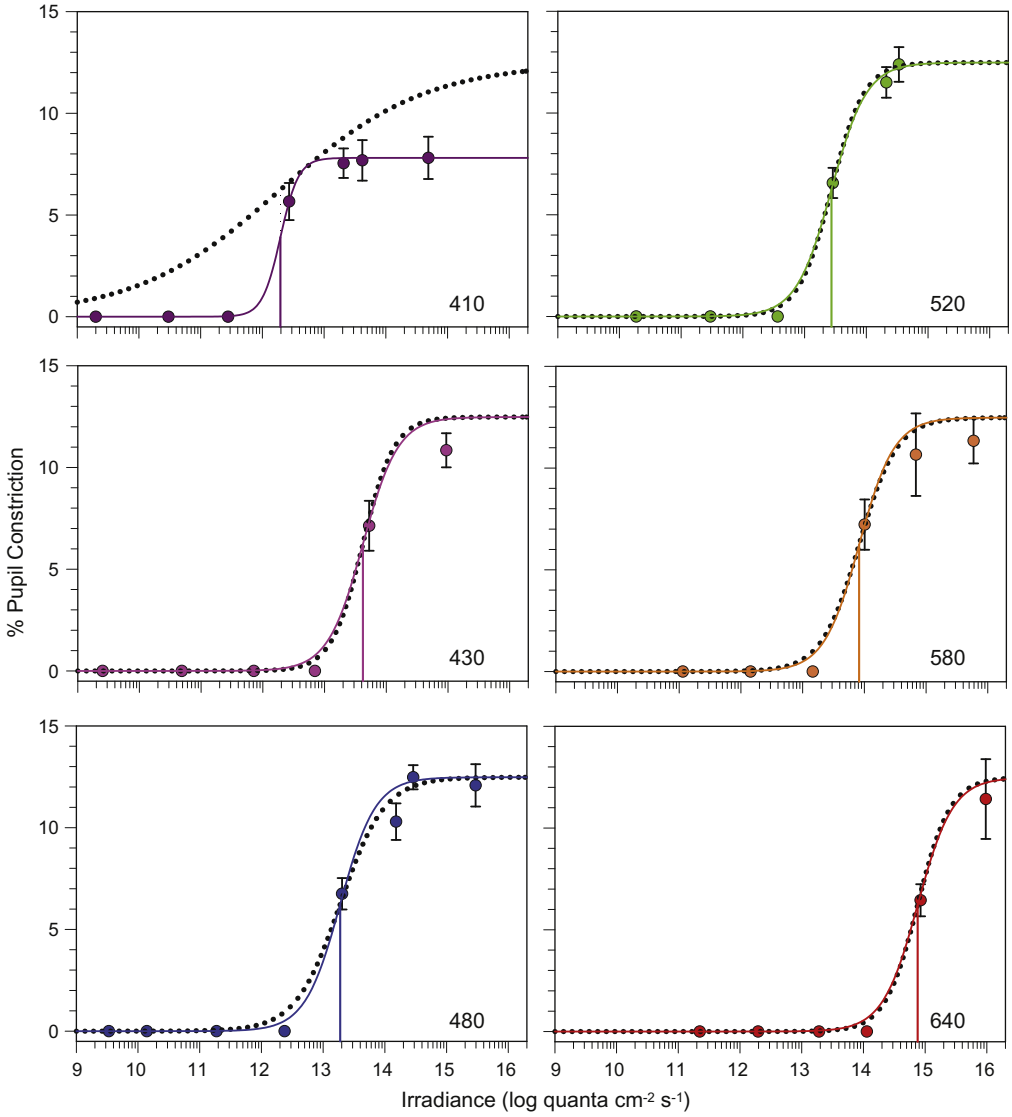

Fig. 7. Pupilloconstrictions versus irradiance on logarithmic scale. Means ± SEs were determined by taking the difference of normalized pupil sizes during the final 5 min of dark adaptation and light adaptation (cf. Fig. 4). Trial number tested was between 3 and 13 at each intensity level, which generated a sample number (*N*) ranging between 15 and 65. Intensities of light that did not produce significant changes in pupil sizes were plotted as zeros. Hill equations were used to calculate thresholds producing 50% of the maximum (drop down lines). The dotted lines are the curves generated using the maximum found at 480 nm. The solid colored lines for 430 through 640 nm are refitted curves using the average of their slopes, $b = 1.52$; the solid line for 410 nm shows a refitted curve using its own maximum and with a slope ~twice as great, $b = 2.96$. (For interpretation of the references to colour in this figure legend, the reader is referred to the web version of this article.)

Table 5
Fitted values for Hill equations.

Narrow-band filters λ_n with 10 nm, FWHM	Slope constant b ± SE with the maximum pupilloconstriction $a = 12.48\%$ (found using 480 nm)	r^2	Average of slope constants from fits to 430–640 nm	Threshold c ± SE log quanta cm^{-2} s^{-1}	Refitted r^2
410	0.37 ± 0.23	0.58	[a]2.96 ± 0.30	12.29 ± 6.85	1.00
430	1.71 ± 0.91	0.97	1.52	13.62 ± 7.69	0.97
480	1.21 ± 0.33	0.99	1.52	13.28 ± 7.61	0.99
520	1.63 ± 0.38	1.00	1.52	13.44 ± 7.27	1.00
580	1.42 ± 0.61	0.98	1.52	13.92 ± 7.75	0.98
640	1.64 ± 0.62	0.99	1.52	14.88 ± 7.49	0.99

[a] Slope constant found for 410 nm and best refitted with its maximum pupilloconstriction, $a = 7.81\%$.

4.3. Spectral sensitivity

Experiments using broad-band spectral lights (Figs. 2 and 3, Tables 1 and 2) show that hemisected eyes remain responsive and viable for at least up to 70 min after the first light adaptation. Experiments using narrow-band filtered lights at different intensities (Fig. 5) generated an action spectrum that could provide a signature for hypothesizing a candidate photopigment at the source of the PMR (Fig. 9). Relative sensitivity was determined from the log reciprocals of thresholds (Fig. 7 and Table 5) and plotted as a function of wavelength (Fig. 9A, round data symbols). Analysis of the fits to Hill equations (Peirson et al., 2005) revealed two peaks

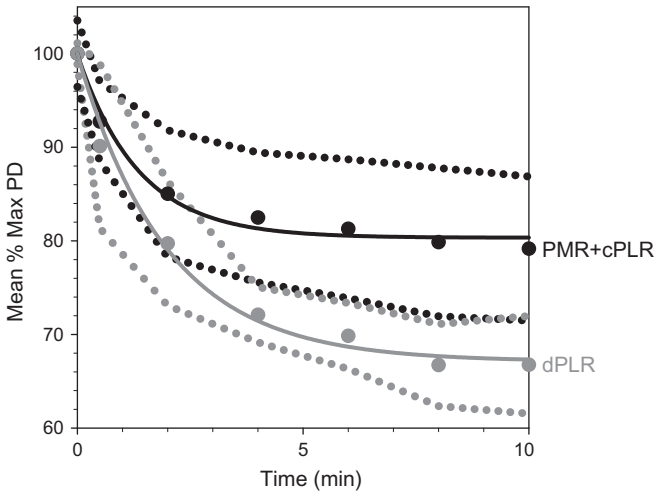

Fig. 8. Additive model for the dPLR, PMR + cPLR. Summed result (black round data symbols) of the PMR (shown in Fig. 1, bottom) added to the cPLR is plotted and compared to the observed dPLR (gray round data symbols). The data for the cPLR was obtained empirically using the results from Dearworth et al. (2010). A rise to maximum time constant equation $y = y_0 + a(1 - e^{-t/\tau})$ was used to generate the data with τ = 1.06 min, the average for the cPLR values reported in that work (Dearworth et al., 2010, Table 3), and a = −13.45%, the value extrapolated from a log/linear plot of cPLR versus light intensity (Dearworth et al., 2010, Fig. 6). The summation was then best fitted (black solid line) with a time constant equation (a = −19.67%, τ = 1.34 min, r^2 = 0.99). Fitting of the dPLR with its curve (gray solid line) is also replotted (cf. Fig. 1, bottom). Dotted lines (black and gray) are 95% confidence limits for the data sets.

of sensitivity, one occurring at 410 nm and a second one at 480 nm that displayed univariance for wavelengths extending from 430 to 640 nm (Table 5).

Nomograms of several visual pigments associated with controlling iris contractions were compared to the action spectrum. In frog, the spectral sensitivity of the PMR (Wald, 1949; Alpern & Barr, 1963; Blaustein & Dewey, 1977) has peak sensitivity at 500 nm resembling rhodopsin (Fig. 9A, dotted line). Fig. 9A (long-dashed line) shows the absorption spectra of human cryptochrome (hCRY1) (Hsu et al., 1996). Because of its involvement in sustained slower pupil responses (Gamlin et al., 2007; Lucas, Douglas, & Foster, 2001; Young & Kimura, 2008), presence within iris (Krivoshik & Barr, 2000; Provencio et al., 1998; Kumbalasiri et al., 2007), and since maximum response of turtle PMR was at 480 nm light, melanopsin (Fig. 9A, medium dashed line) was also considered. Whereas the frog has both vitamin A_1 and A_2 photopigments (Reuter, White, & Wald, 1971), turtle is thought to have just vitamin A_2 derived visual pigments (Liebman & Granda, 1971; Loew & Govardovskii, 2001). We therefore also considered porphyropsin (Fig. 9, solid line), the vitamin A_2 derived photopigment found in rod of turtle. Comparisons of the goodness-of-fits to these nomograms showed that porphyropsin matches the data best with PFE = 43.74%, which was ∼1.4 times better than homologous rhodopsin (63.35%). Next best match was followed by cryptochrome (79.88%) and then melanopsin (224.65%).

Vitamin A_1 (Baylor et al., 1987; DeMarco et al., 1992) and A_2 (Govardovskii et al., 2000) templates were fit to the data from 430 to 640 nm for further investigation of photopigment identity. Both the λ_{max} and the vertical offset of the templates were allowed to vary in order to produce the best fit to the data (Fig. 9B). Both templates fit the data well but was ∼two times better for the vitamin A_2 template (Fig. 9B, dotted line: vitamin A_1, λ_{max} = 523.58 nm and offset = 0.14, PFE = 9.74%; Fig. 9B, solid line: vitamin A_2, λ_{max} = 520.55 nm and offset = 0.0002, PFE = 5.95%). Given that the Hill equation fit to the data for 410 nm suggested the involvement of another photopigment, composite functions also were produced

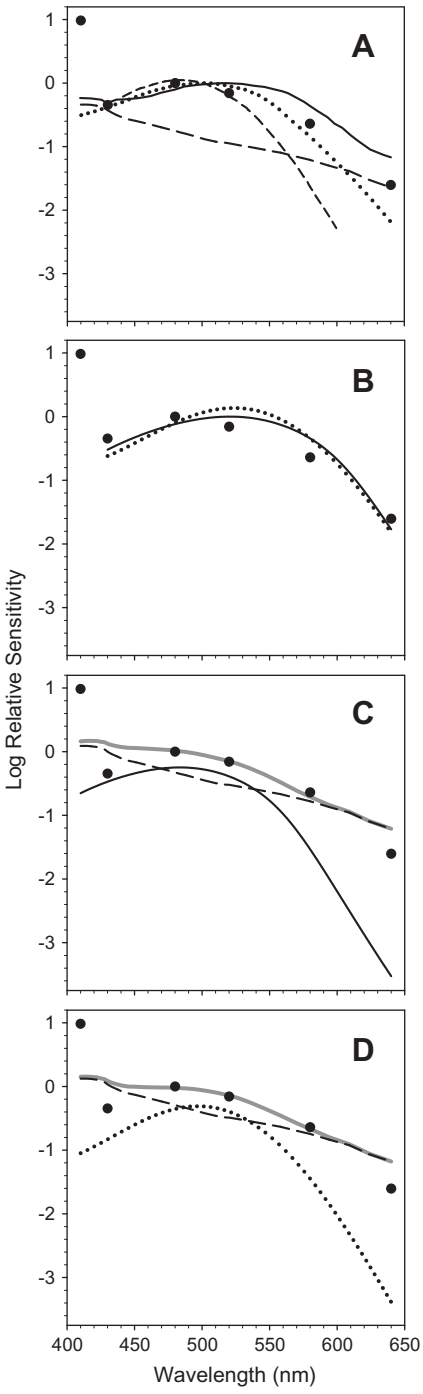

Fig. 9. Relative log sensitivity versus wavelength. Reciprocals of irradiance thresholds were calculated and normalized to the value found at 480 nm. (A) Spectral sensitivity of photointrinsic turtle iris (round symbols) are compared to human cryptochrome (long-dashed line), human melanopsin (medium dashed line), frog rhodopsin (dotted line), and turtle porphyropsin (solid black line). (B) Templates were first fit to the data for 430 through 640 nm: vitamin A_1 (dotted line) and vitamin A_2 (solid black line). Data were fit again with composite functions (solid gray lines) and in this case included the data for 410 nm: (C) composite consisted of human cryptochrome (long-dashed line) with vitamin A_1 template (solid black line) and (D) human cryptochrome (long-dashed line) with vitamin A_2 template (dotted line).

by combining the spectra from multiple sources and then fit to all of the data. In a manner similarly done by McDougal and Gamlin (2010), composites were derived using linear combinations of the absorption spectrum for cryptochrome with vitamin A_1/A_2 templates. To produce the best fit to the data, λ_{max} for the A_1/A_2 tem-

plates and the offsets were allowed to vary. For the vitamin A_1/cryptochrome composite, λ_{max} was 497.02 nm with offsets of −0.31 (vitamin A_1) and 0.46 (cryptochrome) (PFE = 25.96%). The fit for the vitamin A_2/cryptochrome composite was nearly the same (PFE = 25.77%) producing a λ_{max} of 483.44 nm but with lower offsets, −0.25 and 0.43. Interestingly, both vitamin A templates yielded λ_{max} approaching melanopsin.

Rhodopsin and melanopsin are thought to be primary candidates for the frog PMR, and a secondary sensitivity has been identified in the ultra-violet range in eel (Seliger, 1962). In the chick embryo, cryptochrome has been identified as the primary candidate, which has a preferential sensitivity to ultra-violet light and a secondary local peak at 430 nm (Tu et al., 2004). In turtle, the slightly better matches using the vitamin A_2 templates (smaller offsets and lower PFEs) make a compelling argument that one of the pigments involved is opsin-based and derived from vitamin A_2. Because our composite functions fit the data poorly, it seems likely that the other photopigment is novel, or a cryptochrome with an absorbance spectrum significantly different from that used in our model. Further examination of the turtle iris by both biochemical and molecular methods will be necessary to determine the exact identities of these photopigments.

Grants

Funding to support this collaboration was provided by the Department of Biology (Robert S. Chase Fund), the Academic Research Committee through the EXCEL scholarship program, and the Neuroscience Program at Lafayette College.

Acknowledgments

The authors thank Mrs. Paulette McKenna for secretarial support, and Mr. Phil Auerbach for his technical assistance.

References

Armstrong, P. B., & Bell, A. L. (1968). Pupillary responses in the toad as related to innervation of the iris. *The American Journal of Physiology, 214*(3), 566–573.

Barr, L. (1988). Hypersensitivity to light of the iris (Sphincter pupillae) of the albino axolotl (*Ambystoma mexicanum*). *The Journal of Experimental Biology, 137*, 589–596.

Barr, L. (1989). Photomechanical coupling in the vertebrate sphincter pupillae. *Critical Reviews in Neurobiology, 4*, 325–366.

Barr, L., & Alpern, M. (1963). Photosensitivity of the frog iris. *The Journal of General Physiology, 46*, 1249–1265.

Barr, L., & Gu, F. (1987). A Quantitative model of myosin phosphorylation and the photomechanical response of the isolated sphincter pupillae of the frog iris. *Biophysical Journal, 51*, 895–904.

Baylor, D. A., Nunn, B. J., & Schnapf, J. L. (1987). Spectral sensitivity of cones of the monkey *Macaca fascicularis*. *The Journal of Physiology, 390*, 145–160.

Beer, T. (1894). Die akkomodation des fischauges. *Pflügers Arch. ges. Physiol., 58*, 523–650.

Bito, L. Z., & Turansky, D. G. (1975). Photoactivation of pupillary constriction in the isolated in vitro iris of a mammal (*Mesocricetus auratus*). *Comparative Biochemistry and Physiology. A, Comparative Physiology, 50*(2), 407–413.

Blaustein, D. I., & Dewey, M. M. (1977). Localization of antirhodopsin in the frog iris. *Journal of General Physiology, 70*, 2a.

Brown-Séquard, E. (1847). Recherches experimentales sur l'action de la lumiere et sur celle d'un changement de temperature sur l'iris, dans les cinq classes d'animaus vertebres. *Comptes-rendus de l'Académie des sciences, 25*, 482–508.

Brudenall, D. K., Schwab, I. R., & Fritsches, K. A. (2008). Ocular morphology of the Leatherback sea turtle (*Dermochelys coriacea*). *Veterinary Ophthalmology, 11*, 99–110.

Clarke, R. J. (2007). Shaping the pupil's response to light in the hooded rat. *Experimental Brain Research. Experimentelle Hirnforschung. Expérimentation Cérébrale, 176*(4), 641–651.

Dearworth, J. R., Jr., Brenner, J. E., Blaum, J. F., Littlefield, T. E., Fink, D. A., Romano, J. M., et al. (2009). Pupil constriction evoked *in vitro* by stimulation of the oculomotor nerve in the turtle (*Trachemys scripta elegans*). *Visual Neuroscience, 26*(3), 309–318.

Dearworth, J. R., & Cooper, L. J. (2008). Sympathetic influence on the pupillary light response in three red-eared slider turtles (*Trachemys scripta elegans*). *Veterinary Ophthalmology, 11*, 306–313.

Dearworth, J. R., Jr., Cooper, L. J., & McGee, C. (2007). Parasympathetic control of the pupillary light response in the red-eared slider turtle (*Pseudemys scripta elegans*). *Veterinary Ophthalmology, 10*, 106–110.

Dearworth, J. R., Jr., & Granda, A. M. (2002). Multiplied functions unify shapes of ganglion-cell receptive fields in retina of turtle. *Journal of Vision, 2*, 204–217.

Dearworth, J. R., Jr., Sipe, G. O., Cooper, L. J., Brune, E. E., Boyd, A. L., & Riegel, R. A. L. (2010). Consensual pupillary light response in the red-eared slider turtle (*Trachemys scripta elegans*). *Vision Research, 50*, 598–605.

DeMarco, P., Pokorny, J., & Smith, V. C. (1992). Full-spectrum cone sensitivity functions for X-chromosome-linked anomalous trichromats. *Journal of the Optical Society of America. A, Optics and Image Science, 9*(9), 1465–1476.

Distler, C., & Hoffmann, K.-P. (1986). Anatomie und Physiologie des Nucleus praetectalis olivaris (NPO) der Katze und seine Rolle beim Pupillenreflex. *Verh Dtsch Zool Ges, 79*, 268–269.

Douglas, R. H., Harper, R. D., & Case, J. F. (1998). The pupil response of a teleost fish, *Porichthys notatus*: Description and comparison to other species. *Vision Research, 38*(18), 2697–2710.

Dvorak, C. A., Granda, A. M., & Maxwell, J. H. (1980). Photoreceptor signals at visual threshold. *Nature, 283*(5750), 860–861.

Fan, T. X., Scudder, C., & Ariel, M. (1997). Neuronal responses to turtle head rotation *in vitro*. *Journal of Neurobiology, 33*, 99–117.

Fontenot, C. L. Jr., (2008). Variation in pupil diameter in North American Gartersnakes (*Thamnophis*) is regulated by immersion in water, not by light intensity. *Vision Research, 48*, 1663–1669.

Gamlin, P. D., McDougal, D. H., Pokorny, J., Smith, V. C., Yau, K.-W., & Dacey, D. M. (2007). Human and macaque pupil responses driven by melanopsin-containing retinal ganglion cells. *Vision Research, 47*, 946–954.

Glaus-Most, L. (1969). Zur Lichtreaktion der isolierten Froschiris. *Revue Suisse De Zoologie; Annales De La Société Zoologique Suisse Et Du Muséum D'histoire Naturelle De Genève, 76*(4), 799–848.

Govardovskii, V. I., Fyhrquist, N., Reuter, T., Kuzmin, D. G., & Donner, K. (2000). In search of the visual pigment template. *Visual Neuroscience, 17*(4), 509–528.

Granda, A. M., Dearworth, J. R., Jr., Kittila, C. A., & Boyd, W. D. (1995). The pupillary response to light in the turtle. *Visual Neuroscience, 12*, 1127–1133.

Guth, E. (1901). Untersuchungen uber die direkte mootorische Wirkung des Lichtes auf den Sphincter pupillae des Aal und Froschauges. *Pflügers Archiv European Journal of Physiology, 85*, 119–142.

Henning, J., Henning, P. A., & Himstedt, W. (1991). Peripheral and central Contribution to the pupillary reflex control in amphibians – Pupillographic and theoretical considerations. *Biological Cybernetics, 64*, 511–518.

Henning, J., & Himstedt, W. (1994). The pathway controlling the pupillary light reflex in urodeles. *Experimental Brain Research, 98*, 412–420.

Henze, M. J., Schaeffel, F., Wagner, H.-J., & Ott, M. (2004). Accommodation behavior during prey capture in the Vietnamese leaf turtle (*Goemys spengleri*). *Journal of Comparative Physiology. A, Neuroethology, Sensory, Neural, and Behavioral Physiology, 190*(2), 139–146.

Hsu, D. S., Zhao, X., Zhao, S., Kazantsev, A., Wang, R.-P., Todo, T., et al. (1996). Putative human blue-light photoreceptors hCRY1 and hCRY2 are flavoproteins. *Biochemistry, 35*, 13871–13877.

Iske, M. S. (1929). A study of the iris mechanism of the alligator. *Anatomical Record, 44*, 57–77.

Kargacin, G. J., & Detwiler, P. B. (1985). Light-evoked contraction of the photosensitive iris of the frog. *The Journal of Neuroscience, 5*, 3081–3087.

Keifer, J., & Houk, J. C. (1991). Role of excitatory amino acids in mediating burst discharge of red nucleus neurons in the *in vitro* turtle brain stem-cerebellum. *Journal of Neurophysiology, 65*, 454–467.

Krivoshik, A. P., & Barr, L. (2000). Force relaxes before the fall of cytosolic calcium in the photomechanical response of rat sphincter pupillae. *American Journal of Physiology. Cell Physiology, 279*(1), C274–80.

Kuchnow, K. P. (1971). The elasmobranch pupillary response. *Vision Research, 11*, 1395–1406.

Kumbalasiri, T., Rollag, M. D., Isoldi, M. C., de Lauro Castrucci, A. M., & Provencio, I. (2007). Melanopsin triggers the release of internal calcium stores in response to light. *Photochemistry and Photobiology, 83*(2), 273–279.

Lau, K. C., So, K.-F., Campbell, G., & Lieberman, A. R. (1992). Pupillary constriction in response to light in rodents, which does not depend on central neural pathways. *Journal of the Neurological Sciences, 113*, 70–79.

Liebman, P. A., & Granda, A. M. (1971). Microspectrophotometric measurements of visual pigments in two species of turtle, *Pseudemys scripta elegans* and *Chelonia mydas*. *Vision Research, 11*, 105–114.

Loew, E. R., & Govardovskii, V. I. (2001). Photoreceptors and visual pigments in the red-eared turtle, *Trachemys scripta elegans*. *Visual Neuroscience, 18*, 753–757.

Loewenfeld, I. E. (1993). The pupil–anatomy, physiology, and clinical applications, Vol. I. Bibliography and index, Vol. II. Detroit, MI: Wayne State University Press.

Lowenstein, O., & Loewenfeld, I. E. (1950). Mutual role of sympathetic and parasympathetic in shaping of the pupillary reflex to light: Pupillographic Studies. *Archives of Neurology and Psychiatry, 64*, 341–377.

Lucas, R. J., Douglas, R. H., & Foster, R. G. (2001). Characterization of a novel ocular photopigment capable of driving pupillary constriction in mice. *Nature Neuroscience, 4*, 621–626.

Magnus, R. (1899). Beiträige zur Püpillarreaktion des Aal und Froschauges. *Ztschr f Biol, 38*, 567–606.

Maxwell, J. H. (1979). Anesthesia and surgery. In M. Harless & H. Morlock (Eds.), *Turtles: Perspective and research* (pp. 127–152). Wiley: New York.

McDougal, D. H., & Gamlin, P. D. (2010). The influence of intrinsically-photosensitive retinal ganglion cells on the spectral sensitivity and response dynamics of the human pupillary light reflex. *Vision Research, 50*, 72–87.

Morris, J. L. (1976). Motor innervation of the toad iris (*Bufo marinus*). *American Journal of Physiology, 231*(4), 1272–1278.

Nilsson, S. (1980). Sympathetic nervous control of the iris sphincter of the Atlantic cod, *Gadus morhua*. *Journal of Comparative Physiology, 138*(2), 149–155.

Nishida, S., & Sears, M. (1970). Fine structure of the anterior epithelial cell layer of the iris of the hen. *Experimental Eye Research, 9*, 241–245.

Northmore, D. P. M., & Granda, A. M. (1991). Ocular dimensions and schematic eyes of freshwater and sea turtles. *Visual Neuroscience, 7*, 627–635.

Oliphant, L. W., Johnson, M. R., Murphy, C., & Howland, H. (1983). The musculature and pupillary response of the great horned owl iris. *Experimental Eye Research, 37*, 583–595.

Peirson, S. N., Thompson, S., Hankins, M. W., & Foster, R. G. (2005). Mammalian photoentrainment: Results, methods, and approaches. *Methods in Enzymology, 393*, 697–726.

Pilar, G., Nunez, R., McLennan, I. S., & Meriney, S. D. (1987). Muscarinic and nicotinic synaptic activation of the developing chicken iris. *The Journal of Neuroscience, 7*, 3813–3826.

Provencio, I., Jiang, G., De Grip, W. J., Hayes, W. P., & Rollag, M. D. (1998). Melanopsin: An opsin in melanophores, brain, and eye. *Proceedings of the National Academy of Sciences of the United States of America, 95*, 340–345.

Reger, J. F. (1966). The fine structure of iridial constrictor pupillae muscle of *Alligator mississippiensis*. *Anatomical Record, 155*, 197–215.

Reuter, T. E., White, R. H., & Wald, G. E. (1971). Rhodopsin and porophyropsin fields in the adult bullfrog retina. *The Journal of General Physiology, 58*, 351–371.

Rubin, L., Eller, P., & Nolte, J. (1986). Fine structure of the photosensitive iris of the toad, *Bufo marinus*. *Journal of Morphology, 188*, 225–238.

Rubin, L., & Nolte, J. (1982). Autonomic innervation and photosensitivity of the sphincter pupillae muscle of two teleosts: *Lophius piscatorius* and *Opsanus tau*. *Current Eye Research, 1*(9), 543–551.

Seliger, H. H. (1962). Direct action of light in naturally pigmented muscle fibers. I. Action spectrum for contraction in eel iris sphincter. *The Journal of General Physiology, 46*, 333–342.

Steinach, E. (1892). Untersuchungen zur vergleichenden physiologie der Iris. *Pfluegers Archiv, 57*, 495–498.

Sun, M., & Bonds, A. B. (1994). Two-dimensional receptive-field organization in striate cortical neurons of the cat. *Visual Neuroscience, 11*, 703–720.

Tu, D. C., Batten, M. L., Palczewski, K., & Van Gelder, R. N. (2004). Nonvisual photoreception in the chicken iris. *Science, 306*, 129–131.

van Herk, A. W. A. (1928). Le retrecissement par eclairage de la pupille de I'iris isole. *Archives Néerlandaises de Physiologie de l'homme et des Animaux, 13*, 534–568.

von Campenhausen, C. (1963). Quantinative Beziehungen zwischen Lichtreiz und Kontraktion des Musculus sphincter pupillae vom Scheibenzungler (*Discoglossus pictus*). *Kybernetik, 1*, 249–267.

von Studnitz, G. (1933). Studien zur vergleichenden physiologie der iris. IV. Reptilien. *Zeitschrift für vergleichende Physiologie, 19*, 632.

Wald, G. (1949). The photochemistry of vision. *Documenta Ophthalmologica, 3*, 94–106.

Walls, G. L. (1942). *The vertebrate eye and its adaptive radiation*. New York: Hafner Publishing Company (1967 facsimile edition).

Weal, R. A. (1956). Observations on the direct effect of light on the irides of *Rana temporaria* and *Xenopus laevis*. *Journal of Physiology, 132*, 257.

Young, J. Z. (1933). Comparative studies on the physiology of the iris-I. Selachians. *Proceedings of the Royal Society of London, Series B, Containing Papers of a Biological Character, 112*(776), 228–241.

Young, R. S., & Kimura, E. (2008). Pupillary correlates of light-evoked melanopsin activity in humans. *Vision Research, 48*, 862–871.

Zucker, R. M., & Nolte, J. (1978). Light-induced calcium release in a photosensitive vertebrate smooth muscle. *Nature, 274*, 78–80.

Zucker, R. M., & Nolte, J. (1981). A search for the photoreceptor in the photosensitive irises of normally pigmented and albino hamsters (*Merocricetus auratus*). *Current Eye Research, 1*, 9–18.